Electromagnetically induced transparency with controlled van der Waals interaction

Huaizhi Wu, Meng-Meng Bian, Li-Tuo Shen, Rong-Xin Chen, Zhen-Biao Yang, Shi-Biao Zheng
Department of Physics, Fuzhou University, P. R. China

The transmission of light through cold Rydberg atoms controlled by a second laser beam under the condition of the electromagnetically induced transparency (EIT) has been shown to exhibit highly optical nonlinearity. Here we study this effect with two individually addressed Rydberg atoms under the influence of the interatomic van der Waals interaction. We derive an effectively atomic Raman transition model that can potentially overcome the limits of applications for EIT with atoms of the ladder-type level configuration. By probing one of the atoms, we observe four doublets of absorption induced by the Autler-Townes (AT) splitting and van der Waals interaction. In particular, we find that the EIT center keeps unshifted compared with the case of interatomic interaction free, which demonstrated that the interference among the multiple transition channels is basically destructive. The EIT with controlled Rydberg-Rydberg interaction among few atoms provides a versatile tool for engineering the propagation dynamics of light.

PACS numbers: 42.50Gy, 32.80Ee, 42.50Hz

arXiv:1403.5724v1 [quant-ph] 23 Mar 2014

Dipole-dipole interaction or van der Waals (vdW) interaction between atom pairs being excited to high-lying Rydberg states has recently attracted much attention for its potential applications in quantum information processing [1, 2], many-body quantum simulation [3–7] and nonlinear optics [8–10]. In the context of nonlinear optics, many efforts were dedicated to map Rydberg-Rydberg interaction onto optical field using EIT [11–14]. The interatomic interaction within a Rydberg atomic vapour or cold Rydberg gas can give rise to observable highly optical nonlinearity [11] and nonlocal optical effect [15] as well as new type of photonic quantum gas [16] under conditions of EIT. Moreover, the enhanced optical nonlinearity promises engineering of photonic dissipative many-body dynamics [17] and observation of photon-photon interaction towards the few photons regime [13, 18, 19], where all-optical quantum computation can be realized even at the single-photon level [10]. It has also been recognized that the interatomic interaction modified photon correlation has a significant back action on the Rydberg atom statistics [20]. Most of the EIT schemes involved Rydberg atoms with the ladder-typed level structure, where the coherence is induced between a ground state and a Rydberg state via an intermediate excited state [8–20].

In addition to the studies towards controlling the propagation dynamics, the observation and mastering of the coherent dynamics among few Rydberg atoms in the limit of strong blockade or partial blockade has been an essential goal for the dipole blockade based quantum information processing [1, 2, 21]. Remarkable experimental advance has been recently made for the realization of two-qubit quantum entanglement [22, 23] and quantum gates [24, 25] via join or individual laser steering. In particular, by controlling the interatomic distance, the characteristic C_6/R^6 dependence of the vdW interaction strength between two interacting Rydberg atoms of the interatomic separation R has been observed directly by tracking the time-dependent collectively coherent dynamics [23]. It thus becomes very promising for studying quantum effects and nonlinear optical phenomena with well-localized Rydberg atoms prepared in well defined quantum state [26–28].

Here, we propose a EIT scheme with two interacting four-level Rydberg atoms in the limit of partial blockade. The Rydberg state independently couples to two hyperfine ground states (with the transition between them being dipole-forbidden) by dispersively interacting with the probe and coupling laser beams via two-photon transition processes. This leads to a reduced atomic level structure of the Lambda configuration referred to as effective Raman transition model, which allows for observing a coherence induced between two ground states [29] and therefore overcomes the limits of the ladder configuration for applications [30]. We assume the two atoms can be separately steered and one of them (the probe atom) is uniquely selected to interact with the probe laser beams. The other atom (the control atom) interacting only with the coupling field modulates the propagation of the probe field (through the probe atom) via the tunable vdW interaction. This is in particular facilitated by the coupling of the Rydberg level with the long-lived ground states. We find that the Rydberg-Rydberg interaction strength can be directly mapped onto the optical absorption spectra, which consist of four absorption doublets arising from both the interatomic interaction and the AT splitting induced by atom-laser coupling at the control site. The absorption spectra display a very striking feature that the location of the EIT center remains unchanged compared with the single-atom EIT scheme as the interatomic interaction energy increases, which stems from the destructive quantum interference among all the transition channels.

The setup for the Rydberg-EIT proposal, as schematically shown in Fig.1(a), involves two ^{87}Rb atoms located in separated optical traps (denoted as control site

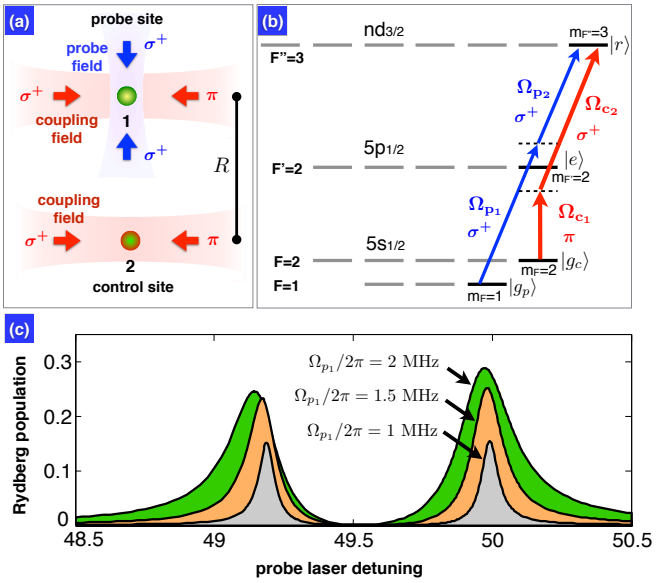

Figure 1. (a) Sketch of setup. (b) Atomic level structure and laser addressing scheme. The level structure are the Zeeman substates of the two hyperfine ground states $F = 1, 2$ of $5s_{1/2}$, the excited state $F' = 2$ of $5p_{1/2}$ and $F'' = 3$ of the high-lying Rydberg state $nd_{3/2}$. A π polarized laser beam red-detuned to the $|F = 2, m_F = 2\rangle \rightarrow |F' = 2, m_{F'} = 2\rangle$ transition and a σ^+ polarized laser beam blue-detuned to the $|F' = 2, m_{F'} = 2\rangle \rightarrow |F'' = 3, m_{F''} = 3\rangle$ transition together act as the coupling channel. While the probe scan is implemented by two σ^+ polarized laser beams blue-detuned to the $|F = 1, m_F = 1\rangle \rightarrow |F' = 2, m_{F'} = 2\rangle$ transition and red-detuned to the $|F' = 2, m_{F'} = 2\rangle \rightarrow |F'' = 3, m_{F''} = 3\rangle$ transition, respectively. (c) The Rydberg spectra without interatomic interaction for increasing probe Rabi frequencies Ω_{p_1,p_2}. The resonance peaks are displaced due to the Stark shifts induced by the coupling and probe laser beams. Parameters are $\Delta_{p_2} = 2\pi \times 50$ MHz, $\Delta_{c_1} = \Delta_{c_2} = 2\pi \times 1$ GHz, $\Omega_{c_1} = \Omega_{c_2} = 2\pi \times 20$ MHz, and $(\gamma_{ec}, \gamma_{ep}, \gamma_r)/2\pi = (3, 3, 0.1)$ MHz.

and probe site) giving access to individual laser addressing [23, 25]. The coupling field, consisting of two laser beams with π polarization and σ^+ polarization respectively, irradiates the pair of atoms and strongly drives the atomic transition from the ground state $|g_c\rangle = |5s_{1/2}, F = 2, m_F = 2\rangle$ to the high-lying Rydberg level $|r\rangle = |nd_{3/2}, F'' = 3, m_{F''} = 3\rangle$ mediated by the excited state $|e\rangle = |5p_{1/2}, F' = 2, m_{F'} = 2\rangle$. The EIT spectroscopy is probed with another two σ^+ polarized laser beams just shining on the probe site and scanning across the $|g_p\rangle = |5s_{1/2}, F = 1, m_F = 1\rangle \rightarrow |r\rangle$ atomic resonance while the C_6/R^6 dependent vdW interaction between the atoms emerges (see caption of the Fig. 1 for details) [23]. The spontaneous decay rates for the atomic transitions $|r\rangle \rightarrow |e\rangle$, $|e\rangle \rightarrow |g_c\rangle$ and $|e\rangle \rightarrow |g_p\rangle$, are γ_r, γ_{ec} and γ_{ep}, respectively. Note that the probability amplitude for finding the atom in the Rydberg state $|r\rangle$ can be used to evaluate the imaginary part of the linear susceptibility for optical response [31]. Therefore, the Rydberg spectra, i.e. the Rydberg population for the atom at the probe site versus the probe laser detuning from two-photon resonance will be detailedly studied here.

In the rotating frame of the atomic bare energies, the dynamics of the two-atom system is governed by the Hamiltonian (set $\hbar = 1$)

$$\begin{aligned}\mathcal{H} = &(\Omega_{p_1}^* e^{-i\Delta_{p_1}t}|g_p\rangle\langle e| + \Omega_{p_2} e^{-i\Delta_{p_2}t}|r\rangle_{11}\langle e| \\ &+ \Omega_{c_1} e^{-i\Delta_{c_1}t}|e\rangle_{11}\langle g_c| + \Omega_{c2}^* e^{-i\Delta_{c_2}t}|e\rangle_{11}\langle r| \\ &+ \Omega_{c_1} e^{-i\Delta_{c_1}t}|e\rangle_{22}\langle g_c| + \Omega_{c2}^* e^{-i\Delta_{c_2}t}|r\rangle_{22}\langle e| \\ &+ H.c.) + \mathcal{V}(R)|r\rangle_1|r\rangle_{22}\langle r|_1\langle r| \end{aligned} \quad (1)$$

with the attractive potential [32, 33]

$$\mathcal{V}(R) = -\frac{C_6}{R^6}, C_6 > 0, \quad (2)$$

where $\Delta_{p_1} = \omega_e - \omega_{g_p} - \omega_{p_1}$, $\Delta_{p_2} = \omega_{p_2} - \omega_r + \omega_e$, $\Delta_{c_1} = \omega_{c_1} - \omega_e - \omega_{g_c}$, $\Delta_{c_2} = \omega_r - \omega_e - \omega_{c_2}$, and Ω_y $(y = p_1, p_2, c_1, c_2)$ are atom-laser coupling strengths for the related atomic transitions as indicated in the Fig. 1(b). The atoms are assumed to identically interact with the coupling laser field. For the dispersive regime $\Omega_y \ll \Delta_y$ $(y = p_1, p_2, c_1, c_2)$, defining the *two-photon probe detuning* $\delta_p = \omega_p - (\omega_r - \omega_{g_p})$ $(\omega_p = \omega_{p_1} + \omega_{p_2})$ and coupling detuning $\delta_c = \omega_c - (\omega_r - \omega_{g_c})$ $(\omega_c = \omega_{c_1} + \omega_{c_2})$ and using the time-averaging method [34], we finally pass to a new interaction Hamiltonian in the rotating frame with respect to $\mathcal{H}_0 = \sum_{k=1,2}\sum_{x=g_p,g_c,r}\mu_{k,x}|x\rangle_{kk}\langle x|$ (with $\mu_{1,g_p} = \delta_p + \alpha_1$, $\mu_{1,g_c} = -\delta_c + \alpha_1$, $\mu_{1,r} = \alpha_1$, $\mu_{2,g_p} = 0$, $\mu_{2,g_c} = -\delta_c + \alpha_2$, $\mu_{2,r} = \alpha_2$, $\alpha_1 = \frac{|\Omega_{c_2}|^2}{\Delta_{c_2}} - \frac{|\Omega_{p_2}|^2}{\Delta_{p_2}}$, and $\alpha_2 = \frac{|\Omega_{c_2}|^2}{\Delta_{c_2}}$)

$$\begin{aligned}\mathcal{H}_e = &\varepsilon_p|g_p\rangle_{11}\langle g_p| + \varepsilon_c|g_c\rangle_{11}\langle g_c| + \varepsilon_c'|g_c\rangle_{22}\langle g_c| \\ &+ (\lambda_p|r\rangle_{11}\langle g_p| + \lambda_c\sum_{k=1,2}|r\rangle_{kk}\langle g_c| + H.c.) \\ &+ \mathcal{V}(R)|r\rangle_1|r\rangle_{22}\langle r|_1\langle r|, \end{aligned} \quad (3)$$

where $\lambda_p = -\frac{1}{2}\Omega_{p_1}^*\Omega_{p_2}(\frac{1}{\Delta_{p_1}} + \frac{1}{\Delta_{p_2}})$, $\lambda_c = -\frac{1}{2}\Omega_{c_1}^*\Omega_{c_2}(\frac{1}{\Delta_{c_1}} + \frac{1}{\Delta_{c_2}})$, $\varepsilon_p = \beta_1 - \delta_p$, $\varepsilon_c = \beta_2 + \delta_c$, $\varepsilon_c' = \beta_3 + \delta_c$, $\beta_1 = \frac{|\Omega_{p_2}|^2}{\Delta_{p_2}} - \frac{|\Omega_{p_1}|^2}{\Delta_{p_1}} - \frac{|\Omega_{c_2}|^2}{\Delta_{c_2}}$, $\beta_2 = \frac{|\Omega_{c_1}|^2}{\Delta_{c_1}} - \frac{|\Omega_{c_2}|^2}{\Delta_{c_2}} + \frac{|\Omega_{p_2}|^2}{\Delta_{p_2}}$, and $\beta_3 = \frac{|\Omega_{c_1}|^2}{\Delta_{c_1}} - \frac{|\Omega_{c_2}|^2}{\Delta_{c_2}}$. The system is now described by the time independent interaction Hamiltonian corresponding to an effective three-level Raman (TLR) model, which has been verified numerically to be effective. Since the atoms interact dispersively with the laser beams, the population of the intermediate state $|e\rangle$ approximates $\sum_y(\Omega_y/\Delta_y)^2$ and can be ignored without considering dissipation.

The density operator ρ for the two-atom system [Eq. (3)] can be expressed by a 9×9 matrix. For a given set of parameters, the full dynamics including atomic spontaneous emission is calculated from the master equation with the Lindblad form

$$\dot{\rho} = \frac{1}{i\hbar}[\mathcal{H}, \rho] + \mathcal{L}_1 + \mathcal{L}_2, \quad (4)$$

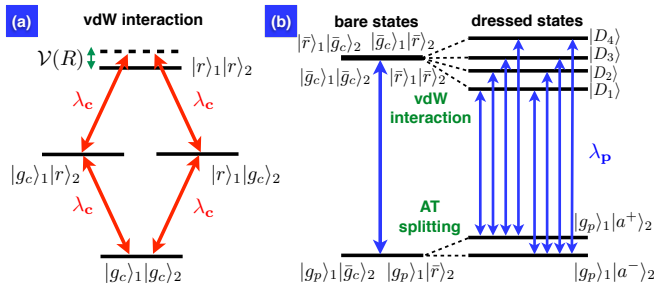

Figure 2. (a) Two-atom transition scheme involving the vdW interaction. The collective Rydberg excited state is shifted according to the attractive potential $\mathcal{V}(R)$. (b) Atomic transition channels induced by the vdW interaction and the AT splitting. The degeneracy of the bare product states consisting of the atoms and lasers are broken due to the vdW interaction while the system state involves Rydberg biexcitation. The ground states and excited states can be well defined by using a picture where the atoms are dressed by the lasers. The probe laser beams then sweep through all the transition channels among the splitted ground states and the shifted dressed excited states.

with

$$\mathcal{L}_j = \frac{1}{2}\sum_{k=c,p}\Gamma_{rk}^{(j)}(2\sigma_{kr}^{(j)}\rho\sigma_{rk}^{(j)} - \sigma_{rk}^{(j)}\sigma_{kr}^{(j)}\rho - \rho\sigma_{rk}^{(j)}\sigma_{kr}^{(j)},$$

where $\sigma_{kr}^{(j)} = |k\rangle_{jj}\langle r|$, $\Gamma_{rk}^{(j)}$ are effective spontaneous decay rates from the Rydberg level $|r\rangle$ to the ground states and are given by $\Gamma_{rp}^{(1)} \approx \gamma_{ep}\gamma_r/(\gamma_{ec}+\gamma_{ep}+\gamma_r)$, $\Gamma_{rc}^{(1)} \approx \gamma_{ec}\gamma_r/(\gamma_{ec}+\gamma_{ep}+\gamma_r)$, $\Gamma_{rp}^{(2)} = 0$ and $\Gamma_{rc}^{(2)} \approx (\gamma_{ec}+\gamma_{ep})\gamma_r/(\gamma_{ec}+\gamma_{ep}+\gamma_r)$. Note that we have taken into consideration the fact that the population of the intermediate excited state $|e\rangle$ (far off-resonantly coupling to the laser beams) induced by the spontaneous emission of the Rydberg state $|r\rangle$ will quickly decay to the ground states for $(\gamma_{ec},\gamma_{ep}) \gg \gamma_r$ [23]. Thus, the time scale for the dissipative transitions from the Rydberg state to the ground states is dominated by $1/\gamma_r$. We neglect dephasing due to atomic collisions as well as amplitude and phase fluctuations of the laser beams, and concentrate on the effect induced by the vdW interaction. While the probe laser beams are applied, steady states can be found by solving the master equation numerically. Then, the Rydberg spectra is calculated by summing over all the diagonal elements involving the Rydberg population of the atom at the probe site.

(a) The Rydberg spectra without interparticle interaction. We first displace the coupling laser beams away from the control atom [35], then the atoms are free to the long range vdW interaction and are uncorrelated. This corresponds to a single atom EIT scheme involving a Λ-type three-level system, which is simply described by the Hamiltonian

$$\begin{aligned}\mathcal{H}_e^{nv} &= \varepsilon_p|g_p\rangle_{11}\langle g_p| + \varepsilon_c|g_c\rangle_{11}\langle g_c| \\ &+ (\lambda_p|r\rangle_{11}\langle g_p| + \lambda_c|r\rangle_{11}\langle g_c| + H.c.).\end{aligned} \tag{5}$$

The strong non-perturbative coupling creates two dressed states (eigenstates) for $\mathcal{H}_e^{nv}$ given by

$$|d_\pm^{nv}\rangle_1 = [(\frac{\varepsilon_c}{2} \pm \sqrt{\frac{\varepsilon_c^2}{4}+\lambda_c^2})|\bar{g}_c\rangle_1 + \lambda_c|\bar{r}\rangle_1]/\mathcal{N}_\pm, \tag{6}$$

with $\mathcal{N}_\pm$ the normalization factors and the relative eigenenergies $E_\pm^{nv} = \varepsilon_c/2 \pm \sqrt{\varepsilon_c^2/4+\lambda_c^2}$. Here, we have denoted the system states by $|\bar{\varphi}\rangle$ $(\varphi = g_c, r)$, which are product states of the 'bare' atom and the coupling laser field for the sake of clarity. Note that the states of the 'bare' atom are now dressed by the resonant laser field through the AC Stark effect and are separated by $\sqrt{\varepsilon_c^2+4\lambda_c^2}$ (known as AT splitting) [36].

In the limit of perturbative probe (i.e. $\lambda_p \ll \lambda_c$), the atomic transitions $|g_p\rangle_1 \to |d_\pm^{nv}\rangle_1$ are in resonance while the condition $\varepsilon_p = E_\pm^{nv}$ is fulfilled. Therefore, the location of the AT doublet corresponding to two-photon resonant absorption lines are found at the probe detunings

$$\delta_p^{(\pm)}(\omega_p) = \beta_1 + E_\pm^{nv}, \tag{7}$$

contributed together by the Stark shifts induced by the probe field and coupling field. This is verified in the Fig. 1(c), where the Rydberg spectra for $\Omega_{p_1} = \Omega_{p_2}$, $\Omega_{c_1} = \Omega_{c_2}$, and $\Delta_{c_1} = \Delta_{c_2}$ is shown.

The EIT resonance condition [the Eq. (7)] can be derived alternatively from the imaginary part of the linear susceptibility calculated with the Hamiltonian $\mathcal{H}_e^{nv}$ and keeping track of the terms that oscillate with the frequency ω_p [30],

$$\mathrm{Im}[\chi^{(1)}] \propto \frac{(\varepsilon_p-\varepsilon_c)\varepsilon_c\gamma_r}{|\varepsilon_p(\varepsilon_p-\varepsilon_c)-\lambda_c^2-i\frac{1}{2}\gamma_r\varepsilon_c|^2}. \tag{8}$$

In fact, the effect of the total decoherence rates (including the atomic spontaneous emission and the finite linewidth of the laser induced dephasing) on $\mathrm{Im}[\chi^{(1)}]$ can be considered simply by replacing γ_r by total decaying rate [30]. Compared with the original EIT scheme [29], the profile of the spectra here are essentially displaced due to the Stark shift of the Rydberg state mainly induced by the coupling laser field $|\Omega_{c_2}|^2/\Delta_{c_2}$ for weak probe. No broadening of the lines was observed for increasing probe Rabi frequencies [see Fig. 1(c)].

(b) The Rydberg spectra with controlled vdW interaction. While the coupling laser beams irradiate both control and probe sites, the potential admixture of the Rydberg state $|r\rangle$ with $|g_c\rangle$ for both atoms will include the collective Rydberg excitation giving rise to the long range vdW interaction and the partial blockade of the Rydberg biexcitation (the regime we are interested in).

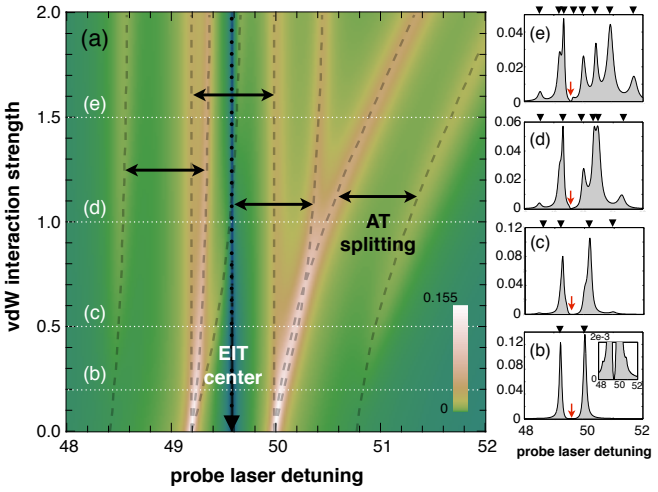

Figure 3. (a) Rydberg population versus probe laser detuning and the vdW interaction. As predicted in Fig.2(b), eight resonant peaks (corresponding to the eight dipole-allowed atomic transition channels) can be resolved in the Rydberg spectra as the vdW interaction strength increases. A detailed calculation by considering two interacting Rydberg atoms with one of them being probed fits well with the numerical results (see the black dash line). (b)-(e) Linecut of the Rydberg spectra along $\mathcal{V}(R)/2\pi = 0.2$ MHz, 0.5 MHz, 1 MHz and 1.5 MHz in (a). The EIT center and the clearly seen absorption peaks are indicated.

Inspired by the case without interparticle interaction, we will adopt the dressed atom picture to gain insight into the dipolar interaction involved EIT phenomenon.

Again for $\lambda_p \ll \lambda_c$, we first concentrate on the coupling channels, in which case the system Hamiltonian narrated by the TLR model reduces to

$$\mathcal{H}_c^v = \varepsilon_c|g_c\rangle_{11}\langle g_c| + \varepsilon_c'|g_c\rangle_{22}\langle g_c| + \sum_{k=1,2}(\lambda_c|r\rangle_{kk}\langle g_c| + H.c.) + \mathcal{V}(R)|r\rangle_1|r\rangle_{22}\langle r|_1\langle r|. \quad (9)$$

The temporal evolution of the system remains in the subspace (written in new notation) spanned by $\bar{\mathcal{R}} = \{|\bar{g}_c\rangle_1|\bar{g}_c\rangle_2, |\bar{g}_c\rangle_1|\bar{r}\rangle_2, |\bar{r}\rangle_1|\bar{g}_c\rangle_2, |\bar{r}\rangle_1|\bar{r}\rangle_2\}$. It is readily to obtain the dressed states (i.e. the eigenstates for H_c^v) for the interacting two-atom system that can be expressed by the superposition of the states within $\bar{\mathcal{R}}$, namely

$$|d_j^v\rangle = \eta_{1,j}|\bar{g}_c\rangle_1|\bar{g}_c\rangle_2 + \eta_{2,j}|\bar{g}_c\rangle_1|\bar{r}\rangle_2 + \eta_{3,j}|\bar{r}\rangle_1|\bar{g}_c\rangle_2 + \eta_{4,j}|\bar{r}\rangle_1|\bar{r}\rangle_2, \quad (10)$$

with the corresponding dressed energies E_j^v $(j = 1,2,3,4)$. Note that the new dressed levels $\{|d_j^v\rangle\}$ have been shifted by $\langle d_j^v|\mathcal{V}(R)|\bar{r}\rangle_1|\bar{r}\rangle_{22}\langle\bar{r}|_1\langle\bar{r}|d_j^v\rangle = |\eta_{4,j}|^2\mathcal{V}(R)$ due to the interparticle interaction, see figure 2(a), and will serve as the collective excited states. On the other hand, for our EIT scheme, the probe atom is initially in $|g_p\rangle_1$ and the control atom is continuously shined by the coupling laser beams, which creates two collective ground states $|g_c\rangle_1|d_\pm^{nv}\rangle_2$ with the separation given by the AT splitting for the initially non-interacting system in the steady state. Hence, the probe laser will scan across the transition channels among the two splitted collective ground states and the four collective excited states. We are able to observe eight resonant absorption peaks arising at the probe detunings divided by two groups

$$\delta_p^{(\pm j)}(\omega_p) = \beta_1 - E_\pm^{nv} + E_j^v, \quad (11)$$

where $|\delta_p^{(+j)} - \delta_p^{(-j)}| = |E_+^{nv} - E_-^{nv}|$ are the AT splittings. For simplicity, we can further assume $\Omega_{c_1} = \Omega_{c_2}$ and $\Delta_{c_1} = \Delta_{c_2}$, and then have $\varepsilon_c = \varepsilon_c' = 0$ without probe scan. In this case, the system states in $\bar{\mathcal{R}}$ are degenerate without the interparticle interaction and the eigenstates for the Hamiltonian involving only the coupling laser field are just the product of the single-atom dressed states $|d_\pm^{nv}\rangle_k$ $(k = 1,2)$ given by Eq. 6. Only when the vdW interaction is included will the atoms become correlated. Then, the degeneracy for $\bar{\mathcal{R}}$ is broken and the dressed states $\{|d_j^v\rangle\}$ including an unshifted dark state $(|\bar{g}_c\rangle_1|\bar{r}\rangle_2 - |\bar{r}\rangle_1|\bar{g}_c\rangle)/\sqrt{2}$ are found. The two-atom probe scheme in this limit is schematically described in Fig. 2(b).

The numerically calculated Rydberg spectra involving the interparticle vdW interaction is presented in Fig. 3. As the vdW interaction strength increases, all the transition channels get more involved and then we can resolve the resonance peaks more clearly; the peak value of the Rydberg spectra reduces accordingly as the blockade effect enhances. All the eight peaks predicted before can be seen at the probe detunings given by $\delta_p^{(\pm j)}(\omega_p)$ while $\mathcal{V}(R)$ becomes comparable with $|E_+^{nv} - E_-^{nv}|$. In between the peaks, there exists nonvanishing Rydberg population except for $\delta_p = \beta_1 + (E_+^{nv} + E_-^{nv})/2$, which is exactly the location of the EIT center found in the interatomic interaction free scheme [see Fig. 3(b)-(e)]. It is striking that the transparency can be observed *in situ* even though the vdW interaction is significant for the two-body dynamics, which then implies that the quantum interference among the multiple transition channels must be destructive. The peaks distribute asymmetrically around the EIT center. On the other hand, the extended profile of the Rydberg spectra allows one to control the absorption of light in a wider range of laser frequency compared with the case without interatomic interaction.

We now turn to a brief discussion of the experimental feasibility. To carry out the EIT scheme proposed here, the atoms must be close enough to experience the vdW interaction, yet far enough apart that one of the atoms can be probed. It is noted that the scheme may be implemented with the new developed setup used for direct measurement of the vdW interaction between two Rydberg atoms [23], where the interaction strength ranged from 0 to 10 MHz can be flexibly tuned by controlling the interatomic separation of a few micrometers. It thus

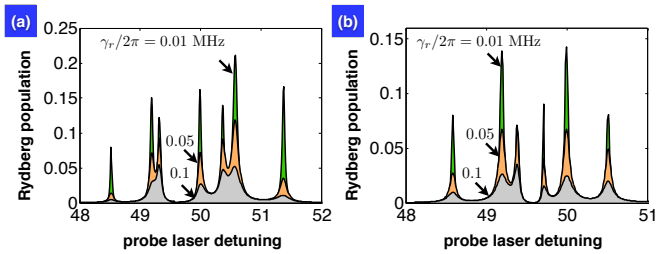

Figure 4. Rydberg spectra for distinct spontaneous emission rates $\gamma_r/2\pi = 0.01$, 0.05, 0.1 MHz, corresponding to different Rydberg levels. The interatomic interaction strengths are (a) $\mathcal{V}(R)/2\pi = 1.1$ MHz and (b) $\mathcal{V}(R)/2\pi = 4$ MHz, respectively. The absorption peaks can be better resolved as γ_r decreases and their locations are only determined by the vdW interaction strength (see Fig. 3).

features the individual addressing of the atoms by applying the the optical-wavelength laser beams focused to a small waist [35, 37]. On the other hand, the Rydberg level $|r\rangle$ with the principal quantum number n has the radiative lifetime scaling as n^3. Therefore, the spontaneous emission rate γ_r of $|r\rangle$ should be much less than that of the intermediate level $|e\rangle$ ($\sim 2\pi \times 3$ MHz) for large n. We have shown the Rydberg spectra for varied γ_r (corresponding to different Rydberg states) in Fig. 4, which depicts that the unshifted resonance peaks can be better resolved as γ_r decreases.

In conclusion, we have studied the EIT phenomena where the interaction of two four-level Rydberg atoms with laser beams can be effectively described by the TLR model. The Rabi oscillation between the ground and Rydberg states allows us to steadily observe EIT under the effect of the vdW interaction. The interatomic interaction induced level shifts accompanied by the AT splitting construct an effective diagram of the atomic transition channels, from which we precisely read out the locations of the peaks (corresponding to two-photon resonant absorption) in the Rydberg spectra. The appearance of the minimal absorption at the position that is exactly the same to the case without interatomic interaction enables us to conclude that the destructive interference preserves even though the vdW interaction is comparable to transition Rabi frequencies. The EIT with controlled vdW interaction may potentially enable modulation of light propagation in a wider range of probe frequency and better understanding of the linear or nonlinear optical response with few photons and few atoms.

This work was supported by the Major State Basic Research Development Program of China under Grant No. 2012CB921601, the National Natural Science Foundation of China under Grants No. 11305037, No. 11347114, and No. 11374054, the Natural Science Foundation of Fujian Province under Grant No. 2013J01012, and the fund from Fuzhou University.

[1] M. Saffman, T. G. Walker, and K. Mølmer, Rev. Mod. Phys. **82**, 2313 (2010).
[2] D. Comparat and P. Pillet, J. Opt. Soc. Am. B **27**, 208 (2010).
[3] H. Weimer, M. Muller, I. Lesanovsky, P. Zoller, and H. P. Buchler, Nat. Phys. **6**, 382 (2010),
[4] J. Honer, H. Weimer, T. Pfau, and H. P. Büchler, Phys. Rev. Lett. **105**, 160404 (2010).
[5] A. W. Glaetzle, R. Nath, B. Zhao, G. Pupillo, and P. Zoller, Phys. Rev. A **86**, 043403 (2012).
[6] M. Höning, D. Muth, D. Petrosyan, and M. Fleischhauer, Phys. Rev. A **87**, 023401 (2013).
[7] B. Olmos, D. Yu, Y. Singh, F. Schreck, K. Bongs, and I. Lesanovsky, Phys. Rev. Lett. **110**, 143602 (2013).
[8] T. Peyronel et al., Nature(London) **488**, 57 (2012).
[9] V. Parigi et al., Phys. Rev. Lett. **109**, 233602 (2012).
[10] O. Firstenberg et al., Nature(London) **502**, 71 (2013).
[11] J. D. Pritchard et al., Phys. Rev. Lett. **105**, 193603 (2010).
[12] D. Petrosyan, J. Otterbach, and M. Fleischhauer, Phys. Rev. Lett. **107**, 213601 (2011).
[13] A. V. Gorshkov, J. Otterbach, M. Fleischhauer, T. Pohl, and M. D. Lukin, Phys. Rev. Lett. **107**, 133602 (2011).
[14] D. Yan, Y.-M. Liu, Q.-Q. Bao, C.-B. Fu, and J.-H. Wu, Phys. Rev. A **86**, 023828 (2012).
[15] S. Sevinçli, N. Henkel, C. Ates, and T. Pohl, Phys. Rev. Lett. **107**, 153001 (2011).
[16] J. Otterbach, M. Moos, D. Muth, and M. Fleischhauer, Phys. Rev. Lett. **111**, 113001 (2013).
[17] A. V. Gorshkov, R. Nath, and T. Pohl, Phys. Rev. Lett. **110**, 153601 (2013).
[18] E. Shahmoon, G. Kurizki, M. Fleischhauer, and D. Petrosyan, Phys. Rev. A **83**, 033806 (2011).
[19] B. He, A. V. Sharypov, J. Sheng, C. Simon, and M. Xiao, arXiv:1401.1540.
[20] C. S. Hofmann et al., Phys. Rev. Lett. **110**, 203601 (2013).
[21] C. Knoernschild et al., Appl. Phys. Lett. **97**, 134101 (2010).
[22] T. Wilk et al., Phys. Rev. Lett. **104**, 010502 (2010).
[23] L. Béguin, A. Vernier, R. Chicireanu, T. Lahaye, and A. Browaeys, Phys. Rev. Lett. **110**, 263201 (2013).
[24] L. Isenhower et al., Phys. Rev. Lett. **104**, 010503 (2010).
[25] X. L. Zhang, L. Isenhower, A. T. Gill, T. G. Walker, and M. Saffman, Phys. Rev. A **82**, 030306 (2010).
[26] M. Weidemüller, Physics **6**, 71 (2013).
[27] A. Vernier, F. Nogrette, T. Lahaye, and A. Browaeys, arXiv:1402.4077.
[28] M. H. Goerz, E. J. Halperin, J. M. Aytac, C. P. Koch, and K. B. Whaley, arXiv:1401.1858.
[29] S. E. Harris, J. E. Field, and A. Imamoğlu, Phys. Rev. Lett. **64**, 1107 (1990).
[30] M. Fleischhauer, A. Imamoglu, and J. P. Marangos, Rev. Mod. Phys. **77**, 633 (2005).
[31] C. Ates, S. Sevinçli, and T. Pohl, Phys. Rev. A **83**, 041802 (2011).
[32] K. Singer, J. Stanojevic, M. Weidemüller, and R. Côté, J. Phys. B At. Mol. Opt. Phys. **38**, S295 (2005).
[33] A. Reinhard, T. C. Liebisch, B. Knuffman, and G. Raithel, Phys. Rev. A **75**, 032712 (2007).
[34] D. James, Fortschr. Phys. **48**, 823 (2000).

[35] E. Urban et al., Nat. Phys. **5**, 110 (2009).
[36] S. H. Autler and C. H. Townes, Phys. Rev. **100**, 703 (1955).
[37] Y. Miroshnychenko et al., Phys. Rev. A **82**, 013405 (2010).